

# A study on the photoconductivity of a set of horizontal Bridgman semi-insulating GaAs ingots

J. JIMENEZ

*Laboratorio de Fisica del Solido, Facultad de Ciencias, Valladolid, Spain*

M. A. GONZALEZ

*Escuela Tecnica Superior de Ingenieros Industriales, Valladolid, Spain*

J. A. DE SAJA

*Laboratorio de Fisica del Solido, Facultad de Ciencias, Valladolid, Spain*

J. BONNAFE

*Laboratoire de Physique des Solides III, Université des Sciences et Techniques du Languedoc, Pl E Bataillon, 34060 Montpellier cedex, France*

---

We report in this paper a study of the photoconductivity of a set of Horizontal Bridgman semi-insulating GaAs samples. In order to obtain steady-state photoconductivity spectra, we measure the photocurrent by a procedure that consists in thermally erasing the typical GaAs photomemory. The thermal evolution, between 80 and 300 K, of the photoconductivity is also obtained. The data so obtained allow us to distinguish clearly a diversity of behaviours between the photoelectronic properties of the different samples, which could not be observed with the conventional photoconductivity technique. The way in which chromium and oxygen impurities are introduced in GaAs, as well as their charge states, seem to be strongly influenced by native defects and background impurities, which play an important role in the compensation mechanism.

---

## 1. Introduction

There is a large interest on the optical and electrical properties of high resistivity GaAs. Several experimental methods are being used in order to investigate its photoelectronic properties [1-4]. These methods include photoconductivity [4, 5], which is a sensitive one in order to characterize the properties of the impurity levels. The photoconductivity technique embraces a variety of parameters involving the interaction between electrons, photons and electric fields; therefore it should be a complex function of the carrier lifetimes, optical cross-sections (photoionization), capture cross-sections (trapping) and of the densities of the different impurity energy levels presents in the material. The photoresponse of the material is very sensitive to the interaction among these param-

eters, hence it is strongly dependent on the time constants.

In this sense the photoconductivity of GaAs, has been the subject of many studies [4-9]. The interpretation of the spectra is difficult because the photoresponse of this material is very sensitive to the thermal and optical exposure histories of the samples. The characteristic long rise and decay times of the photoresponse of semi-insulating GaAs, may induce modifications on the shape of photoconductivity spectrum, depending on the procedure used for measuring it. Thus, we obtain the photoconductivity spectra in a way that at least permits us to reduce in a significant manner these effects if not removing them. In order to do this, thermal erasure of the photomemory has been carried out, as will be explained in Section 2.

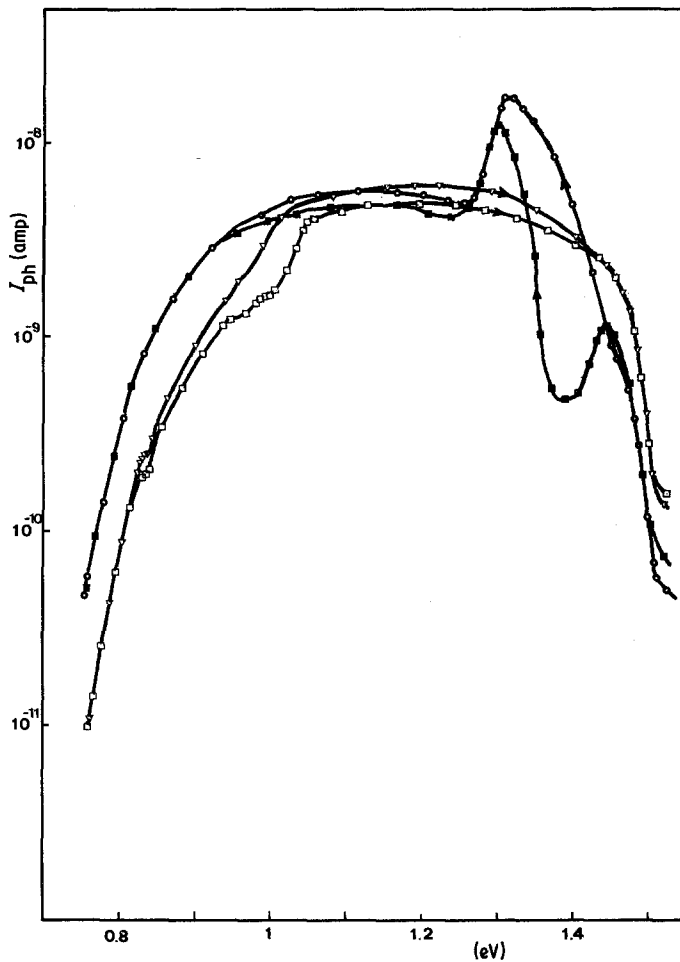


Figure 1 Photocurrent spectra of sample RT527 at 80 K, recorded at continuum light excitation, in the two scanning directions, and for different time intervals between each wavelength measurement: (1)  $h\nu$  (0.7  $\rightarrow$  1.5 eV) ( $\square$ ) 3 min, ( $\nabla$ ) 15 min. (2)  $h\nu$  (1.5  $\rightarrow$  0.7 eV) ( $\blacksquare$ ) 3 min, ( $\bullet$ ) 15 min.

These sort of measurements will allow us to establish differences in the behaviour of a set of bulk semi-insulating GaAs, grown by the Horizontal Bridgman (HB) method, doped with different  $\text{Ga}_2\text{O}_3$  and chromium amounts. Remarkable differences will be observed between the samples, and also the photoconductivity evolution with temperature will be obtained, which will allow us to establish additional differences in the behaviour of the samples.

## 2. Experimental procedure

The obtained photoconductivity spectra should be strongly dependent on the technique used for measuring it [6, 7]. Usual techniques are: continuum light steady-state illumination, and a.c. chopped light illumination. In both cases the shape of the spectrum is strongly dependent on the  $h\nu$  sweeping rate; in Fig. 1 are shown the spectra of a GaAs(Cr, O) sample for different time intervals between each selected monochromatic

light excitations; a strong hysteresis between the two scanning directions is observed.

It is known that the photoconductivity of semi-insulating GaAs is quenched after long excitations with 1.1 eV photons [4, 10, 11] and very long time-constants are found in this spectral range; these transitions are associated to the "O" level, also called EL2 [1, 12, 13], which acts as a deep donor and plays an important role in the compensation mechanism of high resistive GaAs. These effects can be relaxed via a thermally stimulated process. Above 140 K [4, 11], the photomemory is erased and the long time constants are strongly shortened, therefore the steady-state photoconductivity level is reached in shorter times.

The influence of the photomemory effects on the shape of the photoconductivity spectra can be minimized either by thermal erasing or more roughly by a long waiting time between each selected monochromatic excitations.

In this way, measurements were carried out

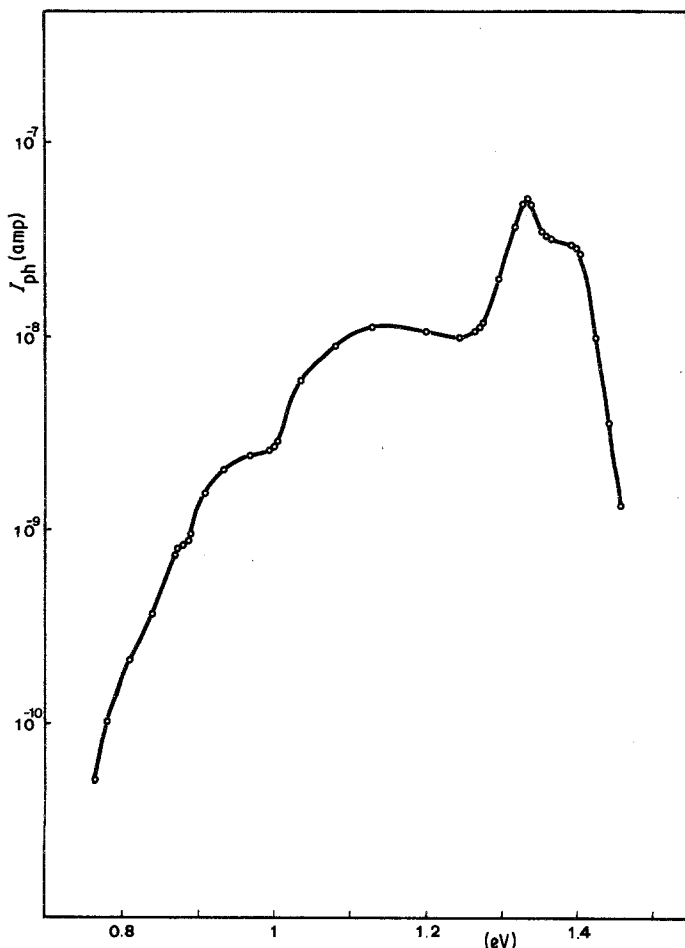


Figure 2 Photocurrent spectra of sample RT527 at 80 K, recorded by the procedure described in Section 2.

with a method that allowed us to obtain the photoconductivity for each selected excitation energy starting out from the equilibrium state by removing the photomemory, previous to each photoconductivity measurement.

The procedure has already been described in a preceding paper [14]. Basically it consists on thermally erasing the photomemory, after a monochromatic light excitation has been fulfilled. An extrinsic photoconductivity spectrum is performed in successive thermal cycles, the following steps being involved in each cycle:

(i) excitation with monochromatic light at low temperatures (liquid nitrogen),

(ii) once the steady-state is reached, the photocurrent is recorded while warming at very slow heating rate,

(iii) when room temperature is reached, the excitation is removed and the sample is cooled in the dark.

These thermal cycles are repeated for each

selected light excitation. The photoconductivity spectra obtained by this procedure are not overshadowed by the photomemory, because the equilibrium populations are thermally restored before each measurement. Furthermore the spectrum can be obtained for any temperature between liquid nitrogen and room temperature.

Obtaining a full photoconductivity spectrum by this procedure is very tedious; in order to obtain it in a shorter time the measurements are made in a small cryostat with a very weak thermal inertia, which allows us to heat from 77 to 300 K in a few minutes. Fig. 2 shows the spectrum obtained by this procedure for the same sample of Fig. 1 (RT527). Important differences can be observed between the spectra of Figs. 1 and 2.

The photoconductivity recording was carried out in the 77 to 300 K temperature range. The swept spectral range includes photon energies between 0.7 and 1.5 eV; in this range optical absorption is homogeneous throughout the sample.

Ohmic contacts were made, after cleaning and polishing the samples, by soldering indium dots and then annealing for a few minutes at 300°C. The applied electric field was chosen in the linear zone of the  $I-V$  curve [15], where homogeneous distribution of the electrostatic field is reasonably acceptable. The measured photocurrent was always significantly higher than the dark current, in the full range considered. Electrical measurements were performed with a 610C Keithley electrometer. The light source used for excitation was a halogen tungsten lamp. A Baush-Lomb grating monochromator was used to select the wavelength.

### 3. Samples

The investigated GaAs samples were bulk platelets (typical dimensions 5 mm × 2 mm × 0.4 mm), cut from ingots grown by the Horizontal Bridgman technique, fabricated by RTC (Radio Technique Compelec). Several kinds of samples were tested, which are characterized by the weights of chromium and Ga<sub>2</sub>O<sub>3</sub> added to the melt. They can be classified into three groups, according to the chromium and Ga<sub>2</sub>O<sub>3</sub> dopant quantities:

1. This group includes samples, which were only intentionally doped with chromium.
2. Samples doped with chromium and Ga<sub>2</sub>O<sub>3</sub>.
3. Samples doped with chromium and Ga<sub>2</sub>O<sub>3</sub>, but with a chromium amount greater than that of group II samples.

Two other samples were studied: an undoped high resistive sample and a Si-O doped sample. The samples with their respective dopants amounts are listed in Table I. It is not well known the way and the proportion in which the dopants are incorporated into the GaAs lattice, (the defect composition varies from sample to sample), even for

TABLE I Chromium and Ga<sub>2</sub>O<sub>3</sub> quantities added to the melt

Group	Samples	Cr/GaAs (weight)	Oxygen (arbitrary units)
I	RT 420	0.00025	—
	RT 490	0.00030	—
	RT 340	0.00035	—
	RT 488	0.000505	—
II	RT 512	0.00020	$A = 1$
	RT 526	0.00020	$B = A \times 2$
	RT 533	0.00020	$C = A \times 3$
	RT 527	0.00020	$D = A \times 25$
III	RT 577	0.00030	$A = 1$
	RT 437	0.00030	$B = A \times 2$
	RT 343	0.00030	$C = A \times 3$

samples cut from the same ingot [16], and it is very dependent on the residual background impurities. Some samples cut from the same ingots as our samples, had been analysed by G. M. Martin, the results of which are reported in [17].

### 4. Thermal equilibrium

The conductivity of a semi-insulating material is determined both by deep and shallow level populations. It has been accepted that the high resistivity of GaAs can be understood by chromium and oxygen compensation of residual shallow levels (donors and acceptors) [2, 18, 19]. Chromium and oxygen impurities would act, respectively, as a deep acceptor and a deep donor [19]. The charge state of deep levels is determined by their density ratio with respect to the density of residual shallow levels [20], which are fully ionized at room temperature. In fact substitutional Cr<sub>Ga</sub> impurity has been observed as Cr<sup>2+</sup>, Cr<sup>3+</sup>, Cr<sup>4+</sup> [21]. Under high pressure conditions [22] or in very heavily doped chromium samples [20] also the Cr<sup>+</sup> charge state has been detected. These features together with the microscopic characteristics of the levels determine the conductivity of the sample. In the set of samples investigated it is evident that the dark current is a complex function of these parameters. The activation energy values obtained from the dark current vary from 0.2 to 0.77 eV. Dark current plots against 10<sup>3</sup>/T are shown in Figs. 3a, b, c and d. Only RT416, 487 and 512 exhibit two slopes. The most important features to be emphasized are the following.

#### 4.1. Group I

These samples have activation energies between 0.4 and 0.55 eV, the smallest values correspond to the most highly Cr-doped samples; furthermore this activation energy decrease is accompanied by a shift of the current plot to higher temperatures (Fig. 3a). This should be related to a change in the type of dominant carriers; in this way it is well known that strong Cr-doped samples are p-type [20].

#### 4.2. Group II

Samples of this group have activation energies of 0.77 eV; only the activation energy of RT512 sample differs from this value. On the other hand, in contrast with group I, the temperature range in which the current is recorded is the same for RT526, 527 and 533 (Fig. 3b). The Fermi level should be pinned at the middle of the gap.

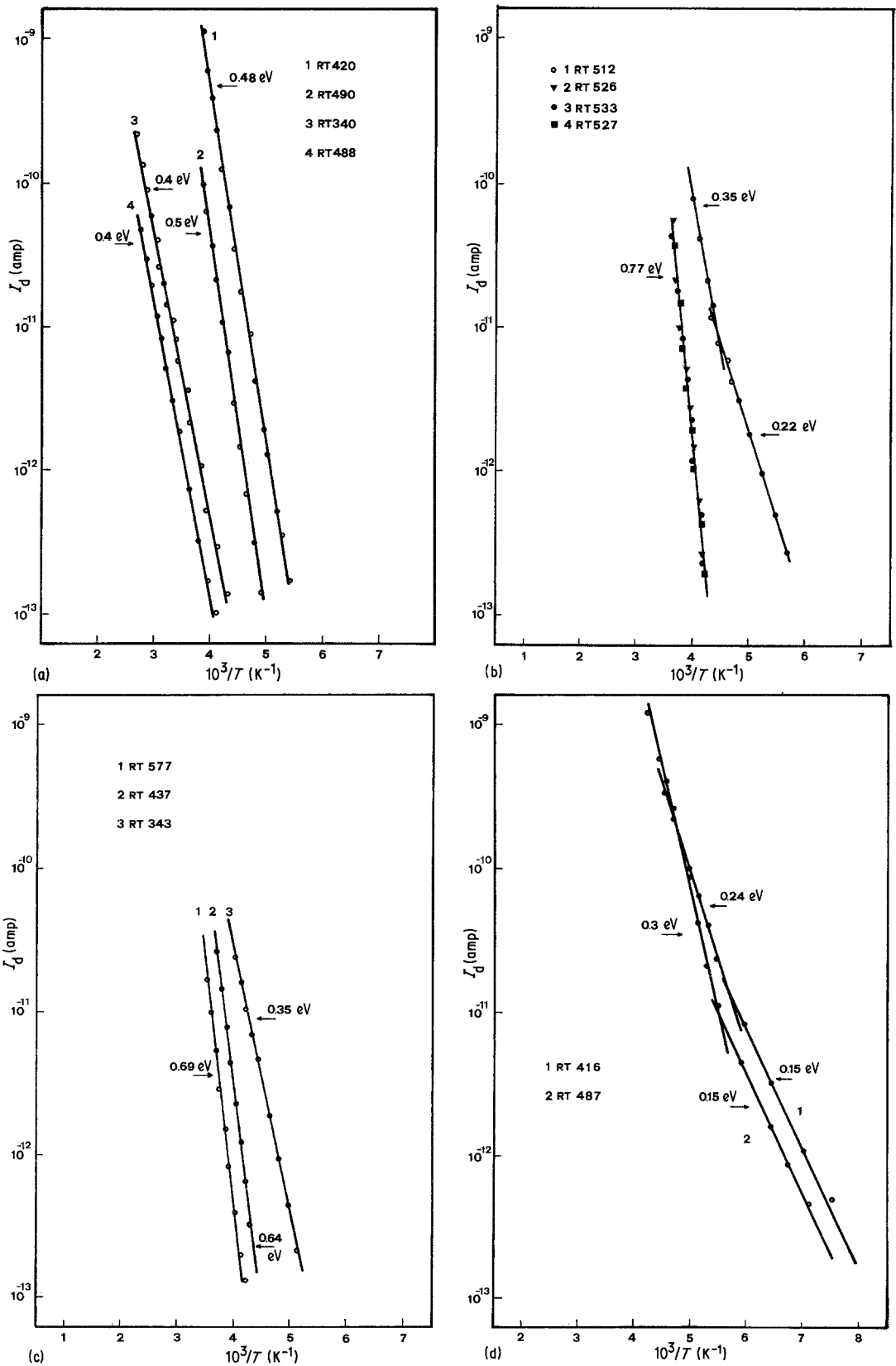


Figure 3 Dark current against  $10^3/T$  ( $I_d$  against  $10^3/T$ ) for the tested samples (a) group I, (b) group II, (c) group III, (d) RT416 and RT487, with their corresponding activation energies.

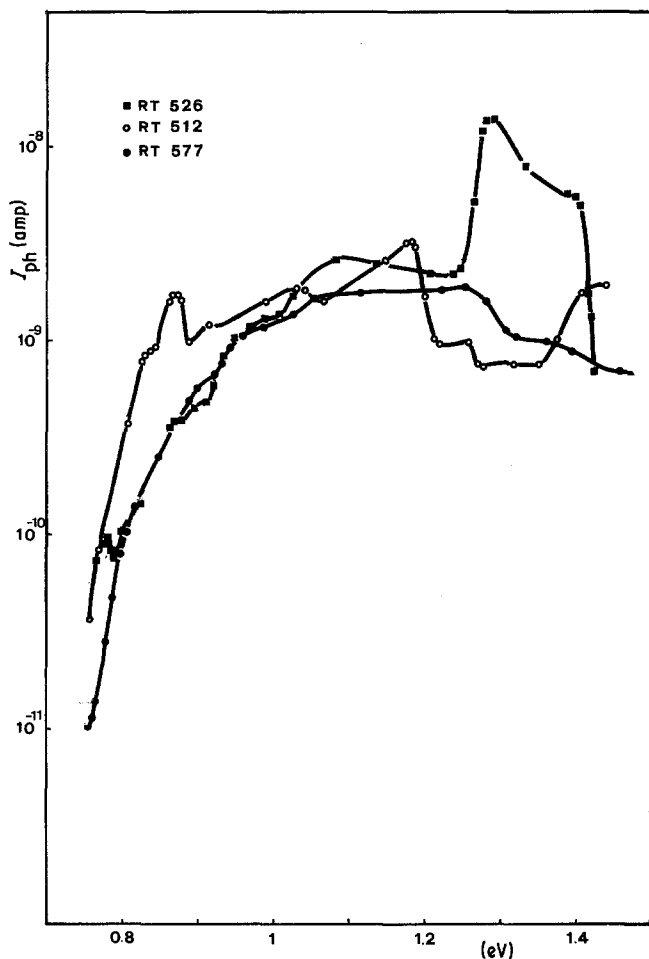


Figure 4 Extrinsic photocurrent spectra at 80 K for some typical samples.

### 4.3. Group III

The values of the activation energies are smaller than those of group II samples; these values are 0.64, 0.69 and 0.35 eV. It is observed that the activation energy decreases when the  $\text{Ga}_2\text{O}_3$  quantity added to the melt increase. A shift of the dark current plot towards lower temperatures is observed in Fig. 3c. The two other tested samples, RT416 and 487, exhibit two slopes, whose values are 0.15 eV below 170 K and 0.24 (RT487) and 0.3 eV (RT416) above 170 K (Fig. 3d). These samples are the least resistive of the lot.

### 5. Photoconductivity

Extrinsic photoconductivity spectra were recorded by the procedure described in Section 2, in the 0.7 to 1.5 eV spectral range and for temperature ranging from 80 to 300 K.

The spectra showed a complex behaviour, and are very dependent on the sample. We observed that the photoresponse time-constants were very

large in samples of group II in the high energy part of the spectrum. However, samples of group I and III had shorter rising and decay times. The extrinsic photoconductivity spectra of several characteristic samples are shown in Fig. 4. The most relevant features of the spectra are the following:

(a) All the samples have a sharp low energy threshold at about 0.75 eV, which indicates that an electronic transition from a level, lying 0.75 eV below the CB, to the  $\Gamma$  minimum of the conduction band is the dominant one in this spectral region. This threshold agrees with other reported photoconductivity results [4, 8, 23]. The level that provides electrons for this electronic transition should be EL2, also reported as the "O" level, because it has been for a long time ascribed to the oxygen impurity [4, 10]. The existence of this threshold in all the samples, independent of the amount of  $\text{Ga}_2\text{O}_3$  added to the melt, indicates that this deep donor level does not originate from the oxygen impurity, but rather that it should be due

to a native defect. Recent papers ascribe this level to the antisite defect  $\text{As}_{\text{Ga}}$ , which would have been formed during the post growth cooling of the ingots [25, 27].

(b) It is well known that other electronic transitions could arise from the EL2 level to the high energy states of the conduction band, namely to the L and X sub-bands, whose minima lie, respectively, 0.29 and 0.46 eV above the minimum of the conduction band [26]. These transitions are the main source of photoconductivity structures in the high energy part of the spectrum. Thus a threshold at 1.03 eV and a broad band at 1.15 eV are frequently observed in the samples, in agreement with other authors [4, 11]. In this part of the spectrum the most important differences between the samples are observed. The longer time constants are related to this part of the spectrum and they are observed in the samples with the strongest photoresponse in this spectral range, RT526, 527, 533, 416.

(c) All the tested samples were intentionally Cr-doped; the most relevant features of the chromium impurity in the photoconductivity spectrum is the existence of a sharp peak at 0.87 eV; which is only clearly observed in the most slightly Cr-doped samples, RT512 and 420. This is a very narrow peak (30 meV in RT512), and it falls sharply for excitation energies higher than 0.88 eV. Due to the technique used for measuring, by means of which the centres are completely refilled before each monochromatic photoconductivity measurement, this fall can not be ascribed to an exhaustion of the centres, but rather to a shortening of the photo-ionization cross-section of the level. This is in agreement with other reported results [4, 9] that attribute this photoconductivity peak to an internal transition of  $\text{Cr}^{2+}$  impurity level, in which the electrons are optically transferred from the  $^5\text{T}_2$  state of the  $\text{Cr}^{2+}$  level to the higher vibronic levels associated with the  $^5\text{E}$  excited state of  $\text{Cr}^{2+}$  level, which are in resonance with the continuum [27]. This peak has been obtained by other authors in photoabsorption [22], photoconductivity [5, 9, 28], EPR [29] and photoluminescence [30] research works.

The 0.87 eV peak is also observed in RT526 and RT527 samples, but in these samples it appears as a very weak one; it is even observed in non-intentionally chromium-doped samples, such as RT416. In conclusion, this peak, which gives evidence of the existence of  $\text{Cr}^{2+}$  charge state of

the chromium impurity, is only detected in samples with small chromium amounts, independent of the  $\text{Ga}_2\text{O}_3$  quantity added to the melt.

(d) A broad photoconductivity band is observed at around 0.95 eV, mainly in the strongly chromium-doped samples. This band is the more relevant one of the photoconductivity spectrum in p-type samples [4, 31]. In n-type samples it is surely overshadowed by the nearest bands, namely those bands arising from EL2 level transitions. This photoconductivity band could arise from an electronic transition between the valence band and a level lying 1 eV above [4].

(e) A weak photoconductivity peak at 0.78 eV is observed in some samples, Fig. 5. Recently Masut *et al.* [32] have reported a similar peak in undoped LEC (Liquid Encapsulated Czochralski) samples. This band has been also obtained in photoluminescence in sample RT533 [33]. The existence of this peak is not related to any particular kind of samples, which seems to indicate that it could be originated by an intrinsic defect arising from the fabrication conditions of the ingot. This is in agreement with the hypothesis of Masut *et al.* [32], who attributes it to dislocations.

## 6. Thermal evolution of photoconductivity

It is well known the relevant role played by temperature on the photoelectronic properties of semi-insulating GaAs [4, 10, 11]: the populations of the levels, as well as their photo-ionization and capture coefficients are very sensitive to temperature variations.

The method that we have used for measuring photoconductivity is tedious, but it provides us the spectrum for any desired temperature, enabling us to achieve a full thermal evolution of the extrinsic photoconductivity.

A great diversity of behaviours might be pointed out in our set of samples. In order to study the thermal evolution of the spectra, we separated the spectral range into two parts, namely below and above 0.9 eV.

### 6.1. Low energy side (0.7 to 0.9 eV)

In this spectral region the thermal dependence of the photoconductivity is not too relevant, Figs. 6 and 7. The most important aspects to be considered are the following.

(a) The 0.75 eV threshold shifts slightly towards lower energies as the temperature increases, with an activation energy dependent on the sample,

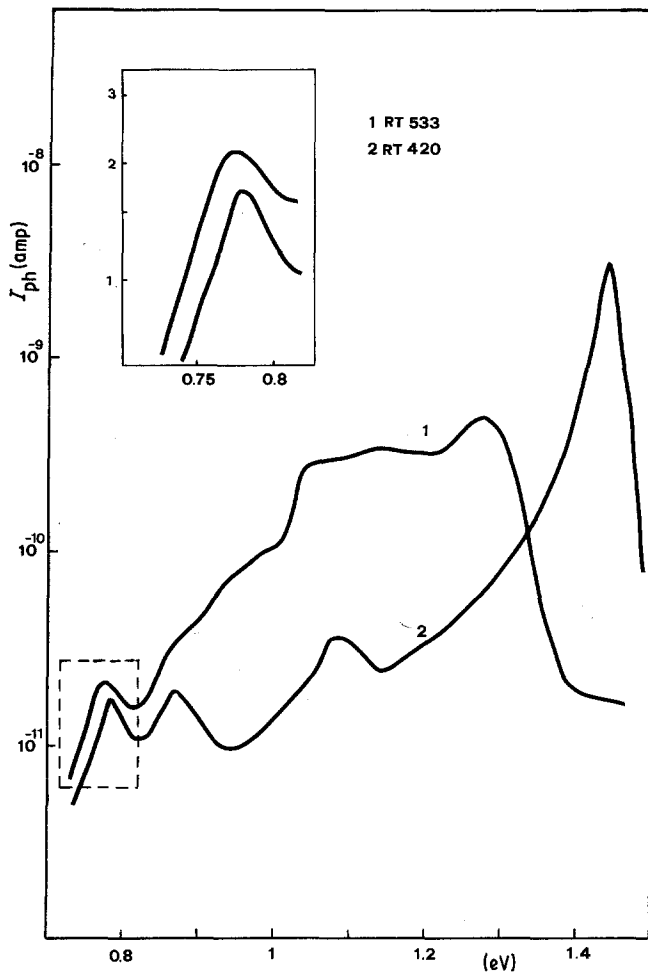


Figure 5 Extrinsic photocurrent spectra at 80 K of RT420 and RT533, with 0.78 eV peak detail.

being 0.024 eV the most frequently obtained value.

(b) The 0.87 eV peak is not broadened by increasing temperature, Fig. 8, which confirms the intracentre nature of the transition.

(c) It is worthwhile to note that a shoulder appears on the spectra when temperature increases, at about 0.83 eV, Figs. 6 and 7. The majority of the samples exhibit this behaviour.

Another aspect to be considered is the evolution of the 0.78 eV peak, which is thermally erased for temperatures above 150 K.

## 6.2. High energy side (0.9 to 1.5 eV)

Contrarily to the low energy part of the spectrum, this zone presents very important thermal effects. The behaviour of the spectra varies strongly from sample to sample. According to it we characterize the samples into several different types:

(i) Samples whose photoconductivity is thermally quenched: these samples are RT 416, 526,

527, 533, and to a lesser degree RT 490 and 343. They exhibit a dramatic thermal quenching of the photoconductivity at about 125 K for energies greater than 1 eV, Fig. 6. When the temperature rises, a slow recovery of the photoconductivity starts. A similar behaviour has been observed by Lin *et al.* [4].

(ii) Other samples, RT 512 and 420, show a slight enhancement of the photoconductivity with increasing temperature. The activation energy for this thermally activated process is 0.024 eV. It should be pointed out that this value agrees with that found for the thermal activation energy of the shift of 0.75 eV photoconductivity threshold (Section 6.1), which confirms that EL2 level could be involved in both transitions.

(iii) When the temperature rises the spectra show their maxima between 0.95 and 1 eV (samples RT 490, 416, 343, 437, 526, 527, 533). For strongly chromium-doped samples, a photoconductivity increase is observed in this spectral region

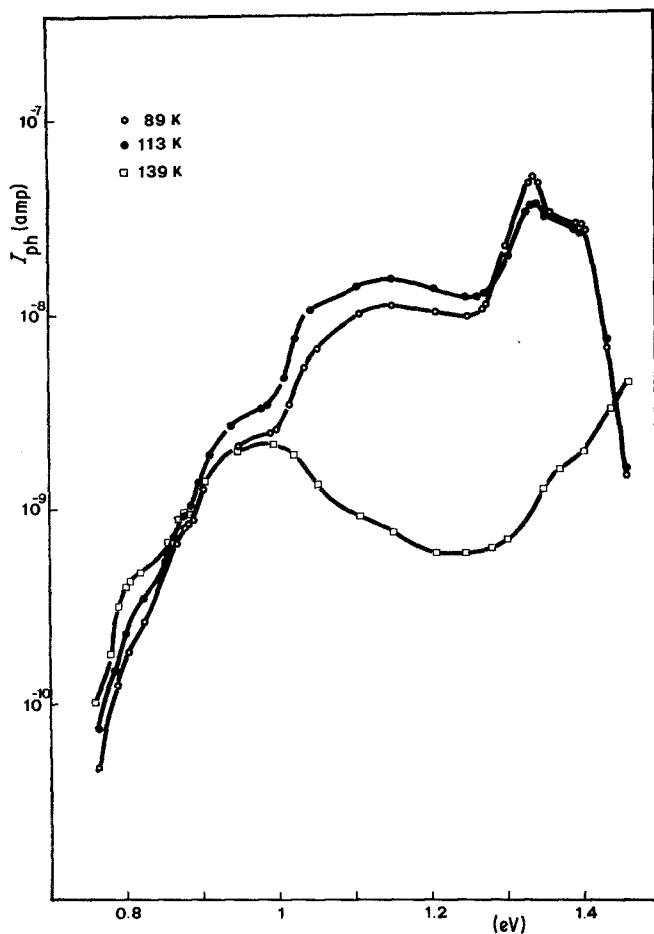


Figure 6 Thermal evolution of the photocurrent spectrum of RT527 sample.

for increasing temperature, Fig. 7. On the contrary for samples that show a thermal photoconductivity quenching (RT 416, 526, 527, 533) the photocurrent level remains constant, although the intensity ratio of this band to the nearest one increases with temperature. These behaviours are dependent on the compensation mechanism of the samples.

## 7. Discussion

As we have said in previous sections the photoconductivity of semi-insulating bulk GaAs is very sample dependent; the compensation mechanism being a complex function of the added chromium and  $\text{Ga}_2\text{O}_3$  and of the background impurities and native defect levels created during the fabrication of the ingots. The density ratio of these levels should determine the electrical and photoelectronic properties of the samples. Because the distribution of the impurities and the creation of the defects are not well controlled in GaAs ingots, the samples

can be very different depending both on the doping and fabrication conditions.

While in previous sections we have shown some characteristic aspects of the experimental photoconductivity results, we shall now consider these results in a systematic way, in order to establish reports between the tested samples.

### 7.1. Chromium impurity

The addition of a fixed quantity of chromium is not sufficient to explain the behaviour of some samples. The dominant charge state of chromium impurity should be determined both by the incorporated chromium amount and by the respective amounts of other impurities and native levels [20, 34]. As we have shown in previous sections the 0.87 eV peak, which is characteristic of the  $\text{Cr}^{2+}$  charge state of chromium impurity, is only obtained in samples for which small chromium amounts were added to the melt. Strongly chromium-doped samples do not exhibit the

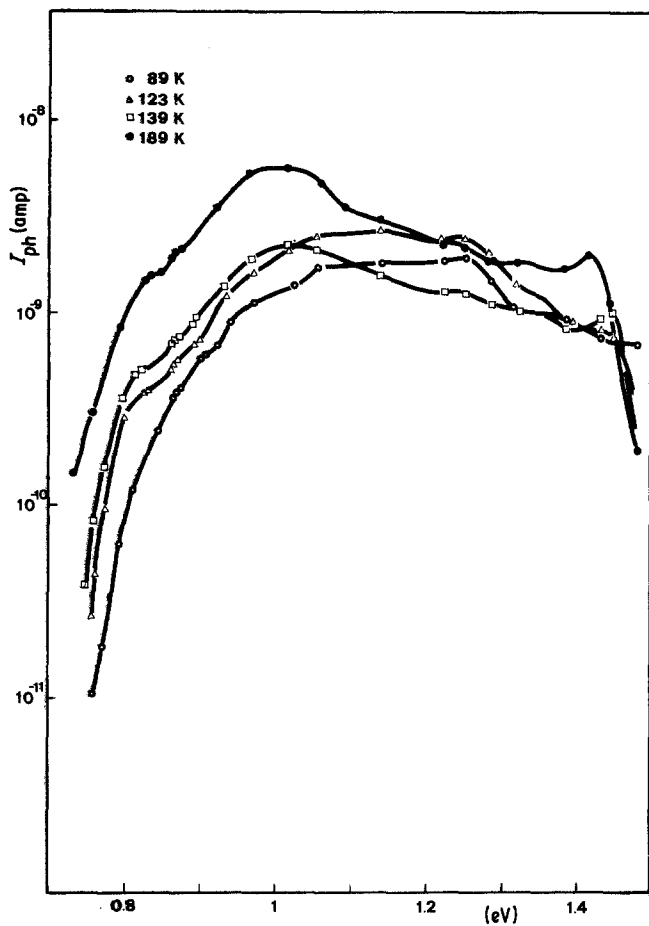


Figure 7 Thermal evolution of the photocurrent spectrum of RT577 sample.

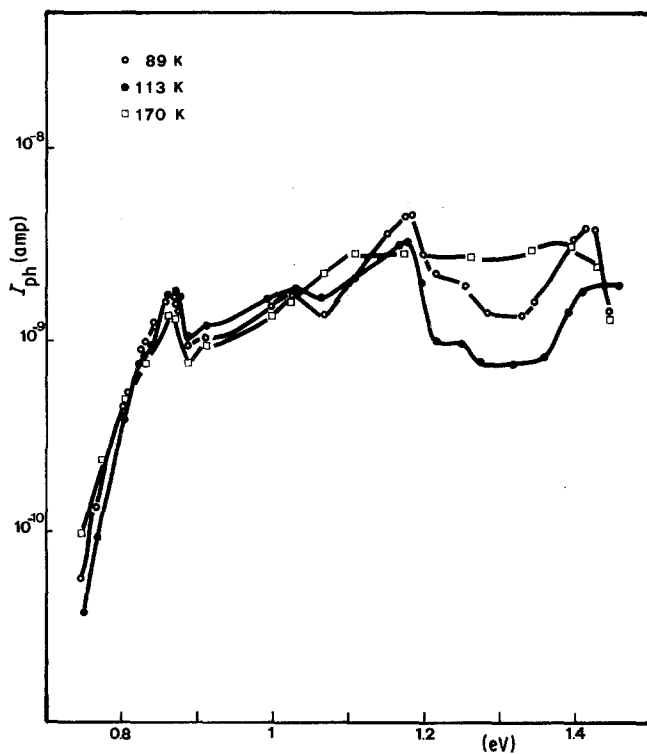


Figure 8 Thermal evolution of the photocurrent spectrum of RT512 sample.

0.87 eV peak, which agrees with the fact that in these samples (in generally p-type)  $\text{Cr}^{2+}$  is not the dominant charge state of the chromium impurity; the Fermi level should be pinned below  $\text{Cr}^{2+}$  ground state, producing stable  $\text{Cr}^{3+}$  or  $\text{Cr}^{4+}$  and reducing therefore the  $\text{Cr}^{2+}$  concentration.

## 7.2. EL2 level

The high energy part of the photoconductivity spectrum can be related to transitions arising from the EL2 level. It is well known that this level is the main electron trap in undoped bulk semi-insulating GaAs [35]. It is usually accepted that this level is responsible for thermal and optical exposure histories observed in high resistivity GaAs [11]. In this way our method of measuring photoconductivity enables us to eliminate photomemory traces, due to previous excitations, before each measurement. Figs. 1 and 2 illustrate the spectra obtained with continuum light illumination and our thermal cycling method. It is observed that the largest differences appear for excitation energies greater than 1 eV, for which photomemory effects are strongest.

As it was seen in Section 6, four samples exhibit a dramatic thermal quenching of the photoconductivity between 120 and 140 K, for energies between 1 and 1.35 eV. Other samples have a different behaviour, namely, RT 512, 420 and 487, which show a slight photocurrent enhancement when the temperature rises. Other samples RT 340, 343, 437 and 488, do not show important variations with temperature change; moreover in these samples no relevant differences are found at 77 K between the spectra recorded at continuum illumination and that obtained by our method. This diversity of behaviours can not be ascribed to any  $\text{Ga}_2\text{O}_3$  added to the melt, i.e. samples 526, 527 and 533 present similar photoconductivity behaviour as well as the same dark Fermi level, Fig. 3b; however, the quantity of  $\text{Ga}_2\text{O}_3$  added to the melt is very different from one sample to another, see Table I. These samples exhibit also an intense photoconductivity band at around 1.3 eV, which appears only after long time excitations and it seems not to be due exclusively to the EL2 level.

## 7.3. Other features

Other important observed properties are the 0.78 eV peak, the 1 eV band and the 0.83 eV shoulder, which were described in previous sections. The former peak (0.78 eV) appears in

some samples, without any apparent relation with the chromium and  $\text{Ga}_2\text{O}_3$  dopant amounts of the samples that exhibit it. This fact suggests that this peak could be due to a native defect, as we indicated in Section 5. It is particularly intense in the undoped RT416 sample.

With respect to the 1 eV photoconductivity band, this peak is especially strong in the strongest chromium doped samples, that is p-type samples; it is also observed in n-type samples for temperatures above 135 K, for which the 1.03 eV photoconductivity band is thermally quenched. These observations suggest that this photoconductivity band could be related to an electron emission from the valence band to an acceptor level lying 1 eV above.

Finally, the 0.83 eV shoulder is only observed when the temperature rises, Figs. 6 and 7. This energy value is equal to the zero phonon line associated to the electronic transition  ${}^5\text{T}_2-{}^5\text{E}$  excited state of  $\text{Cr}^{2+}$  level; however this zero phonon line is only observed in photoconductivity measurements at very low temperatures ( $T < 10\text{ K}$ ) [5]. Furthermore it appears in samples that do not exhibit the characteristic 0.87 eV photoconductivity peak, whose existence evidences the  $\text{Cr}^{2+}$  charge state of chromium impurity. On the other hand, the 0.83 eV shoulder is not observed in the RT512 sample which seems to be the sample that contains the most  $\text{Cr}^{2+}$  of all the samples. These experimental results are contradictory with the assignment of this photoconductivity shoulder to the zero phonon line of  ${}^5\text{T}_2-{}^5\text{E}$  internal transition of  $\text{Cr}^{2+}$  acceptor level; it should be more properly related to thermal variations in the photo-ionization cross-section of EL2-transition.

Table II, summarizes the most relevant features of the extrinsic photoconductivity spectra of the set of Horizontal Bridgman tested samples.

## 8. Concluding remarks

The photoconductivity of semi-insulating GaAs must be carefully measured in order to eliminate the photomemory effects, which prevent a good resolution of the spectra. In this way, we have used a thermal cycling method for measuring the photoconductivity of GaAs, consisting basically in a thermal erase of photomemory, before each monochromatic excitation is carried out. Simultaneously, the thermal evolution of the spectrum is obtained. The resolution of the spectra obtained by this method is very good; complex structures

TABLE II Summary of the most important features observed in the set of samples

Sample	0.75 eV	0.78 eV	0.83 eV ( $T > 120$ K)	0.87 eV	0.95 eV	1.03 eV	1.15 eV	1.3 eV
RT420	threshold	peak		peak		threshold	peak	
RT490	threshold		onset (weak)		band $T > 120$ K band	threshold		
RT340	threshold							
RT488	threshold		onset					*
RT512	threshold			peak	onset (weak)	peak	peak	
RT526	threshold	peak	onset	peak (weak)	broad band	threshold	band	peak
RT527	threshold		onset	peak (weak)	broad band	threshold	band	peak
RT533	threshold	peak	onset	onset (weak)	broad band	threshold	band	peak
RT537	threshold		onset	onset (weak)	broad band	threshold (80 K)		peak(weak) (80 K, 1.25 eV)
RT437	threshold		onset		broad band	threshold (80 K)	broad band (80 K)	
RT343	threshold	peak	onset	onset (weak)	broad band	threshold (80 K)	broad band (80 K)	
RT416	threshold	peak	onset	onset (weak)	band	threshold* (80 K)	peak* (80 K)	
RT487	threshold		onset		band (1 eV, 80 K)			

\*Thermally quenched  $T > 120$  K.

can be observed, revealing strong differences between the samples.

On the other hand, the study of a set of bulk HB GaAs samples, shows a great variety of photo-electronic behaviours, which can not be ascribed to any chromium and  $Ga_2O_3$  dopant composition of the samples. Differences are found between slightly and strongly chromium-doped samples. Any systematic relation has been observed between the  $Ga_2O_3$  quantity added to the melt and the obtained photoconductivity spectra.

The native defects created during sample growth, as well as the background impurities which form complex defects, seem to be determinant in the compensation mechanisms of semi-insulating GaAs. In this way the strong differences between the samples observed in the photoconductivity behaviour could be understood.

### Acknowledgements

The authors would like to acknowledge Mr Poiblaud from RTC Caen for supplying the samples for this work.

### References

1. G. M. MARTIN, G. JACOB, G. POIBLAUD, A.

- GOLTZENE and C. SCHWAB, *Inst. Phys. Conf. Ser.* **59** (1981) 281.
2. G. M. MARTIN, J. P. FARGES, G. JACOB and J. P. HALLAIS, *J. Appl. Phys.* **51** (1980) 2840.
3. P. LEYRAL and G. GUILLOT, 5nd International Conference on Semi-Insulating III-V, Evian (France), April 1982, edited by S. Makram-Ebeid and B. Tuck (Shiva Publishing Ltd, Nantwich, 1982) p. 166.
4. A. L. LIN, E. OMELIANOVSKI and R. H. BUBE, *J. Appl. Phys.* **47** (1976) 1852. A. L. LIN and R. H. BUBE, *ibid.* **50** (1976) 1859.
5. L. EAVES, P. J. WILLIAMS and C. UIHLEIN, *J. Phys. C* **14** (1981) L693.
6. H. G. GRIMMEIS and L. A. LEDEBO, *J. Appl. Phys.* **46** (1975) 2155.
7. F. PRAT and E. FORTIN, *Can. J. Phys.* **50** (1972) 2551.
8. E. H. TYLER, M. JAROS and C. PENCHINA, *Appl. Phys. Lett.* **31** (1977) 208.
9. D. C. LOOK, *Solid State Commun.* **24** (1977) 825.
10. G. P. PEKA, V. A. BRODOVOI, I. I. MISHOVA and L. Z. MIRETS, *Sov. Phys. Semicond.* **12** (1978) 540.
11. G. VINCENT, D. BOIS and A. CHANTRE, *J. Appl. Phys.* **53** (1982) 3643.
12. A. MITONNEAU and A. MIRCEA, *Solid State Commun.* **30** (1979) 157.
13. A. CHANTRE, D. BOIS and G. VINCENT, *Phys. Rev.* **B23** (1981) 5335.
14. J. JIMENEZ, M. A. GONZALEZ, L. F. SANZ and J. BONNAFE, *Phys. Status Solidi (a)* **73** (1982) k189.

15. J. JIMENEZ, J. BONNAFE and J. P. FILLARD, *J. Appl. Phys.* **50** (1979) 1150.
16. J. BONNAFE *et al.*, *Mater. Res. Bull.* **16** (1981) 1193.
17. G. M. MARTIN, G. JACOB, J. P. HALLAIS, F. GRAINGER, B. CLEGG, P. BLOD and G. POIBLAUD, *J. Phys. C.* **15** (1982) 1841.
18. R. ZUCCA, *J. Appl. Phys.* **48** (1977) 1987.
19. P. F. LINDQUIST, *ibid.* **48** (1977) 1262.
20. M. R. BROZEL, J. BUTLER, R. C. NEWMAN, A. RITSON, D. J. STIRLAND and C. WHITEHEAD, *J. Phys. C.* **11** (1978) 1857.
21. G. H. STAUSS, J. J. KREBS, S. H. LEE and E. M. SWIGGARD, *Phys. Rev.* **B22** (1980) 3141.
22. A. M. HENNEL, W. SZUSZKEEWICZ, M. BALKANSKI, G. MARTINEZ and B. CLERJAUD, *ibid.* **B23** (1981) 3933.
23. H. J. STOCKER, *J. Appl. Phys.* **48** (1977) 4583.
24. D. E. HOLMES, K. R. ELLIOT, R. T. CHEN and C. G. KIRKPATRICK, 5nd International Conference on Semi-Insulating III-V, Evian (France), April 1982.
25. J. LAGOWSKI, J. M. PARSEY, M. KAMINSKA, K. WADA and H. C. GATOS, 5nd International Conference on Semi-Insulating III-V, Evian (France), April 1982, edited by S. Makram-Ebeid and B. Tuck (Shiva Publishing Ltd, Nantwich, 1982) p. 19.
26. D. E. APSNES, *Phys. Rev.* **B14** (1976) 5331.
27. D. BOIS and P. PINARD, *ibid.* **B9** (1974) 4171.
28. K. KITAHARA, K. NAKAI, H. SHIBATOMI and S. OKAWA, *J. Appl. Phys.* **50** (1979) 5339.
29. U. KAUFMANN and J. SCHNEIDER, *Solid State Commun.* **20** (1976) 143.
30. G. PICOLI, B. DEVEAUD and D. GALLAND, *J. Phys.* **42** (1981) 133.
31. W. PLEISIEWICZ, *J. Phys. Chem. Solids* **38** (1977) 1079.
32. R. MASUT, J. L. FARVACQUE and C. PENCHINA, *Solid State Commun.* **44** (1982) 1413.
33. P. LEYRAL, private communication (1982).
34. J. S. BLAKEMORE, *J. Appl. Phys.* **53** (1982) 520.
35. G. M. MARTIN, *Appl. Phys. Lett.* **39** (1981) 747.

*Received 10 May  
and accepted 26 July 1983*